
1922—2022

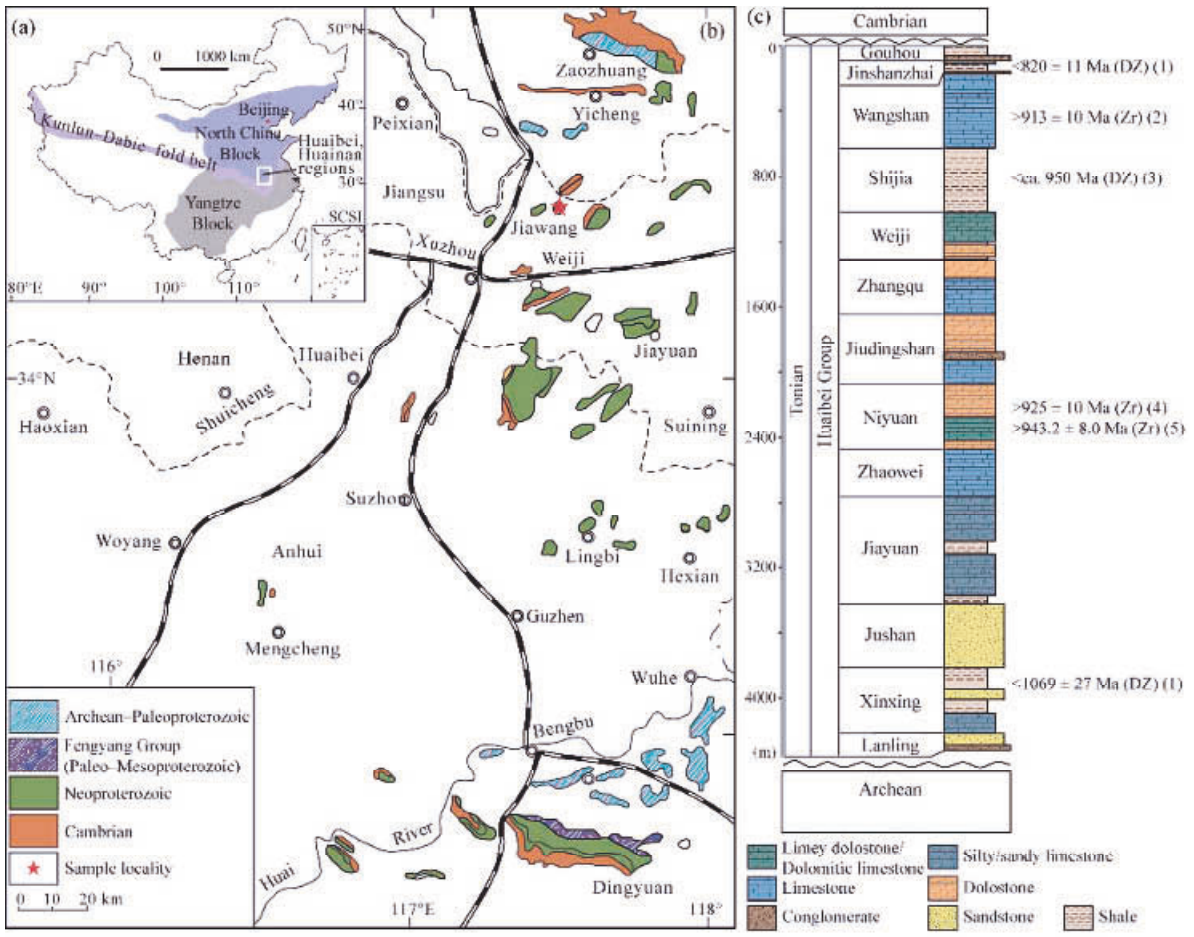

Fig. 1. Geological maps and stratigraphic column.

(a) Simplified geological map showing the location of the North China Block. The white box marks the Huaibei and Huainan regions. SCSI=South China Sea Islands. China basemap after China National Bureau of Surveying and Mapping Geographical Information; (b) geological map of the Huaibei and Huainan regions (white box in Fig. 1a), showing the distribution of Precambrian and lower Cambrian outcrops. The sampling locality is marked by a red star; (c) simplified stratigraphic column of the Huaibei Group in the Huaibei region. Samples of this study came from the Weiji Formation. Modified from Xiao et al. (2014), Wan et al. (2019), and Zhao et al. (2020). By–baddeleyite; DZ–detrital zircon; Zr–magmatic zircon. References for radiometric ages: (1) Yang et al. (2012); (2) Zhu et al. (2019); (3) He et al. (2016); (4) Fu et al. (2015); (5) Zhao et al. (2020).

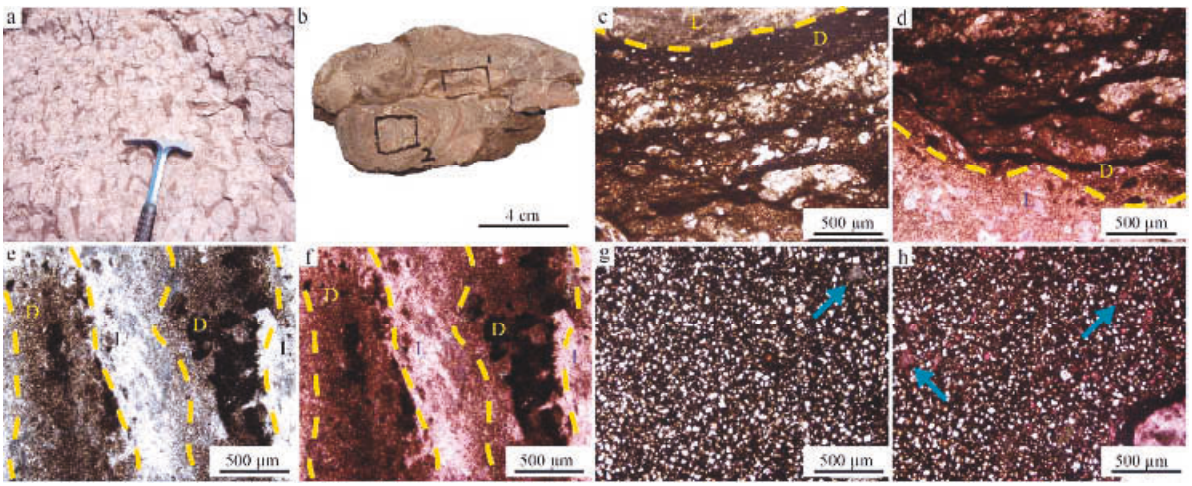

Fig. 2. Stromatolitic and dolomitic limestone with type I dolomitization pattern.

(a–b) Outcrop and hand-specimen photographs showing light-colored columnar stromatolites and red-colored matrix sediment. Boxes in (b) mark areas selected to make thin and thick sections; (c, e, g) transmitted light photomicrographs of petrographic thin sections, showing that dark-colored stromatolitic laminae with crinkled microbial structures (labeled "D" in c–e) and light-colored stromatolitic laminae are composed of sparry calcite (labeled "L" in c and e), whereas the matrix is preferentially dolomitized (g); (d, f, h) transmitted light photomicrographs of ARS-stained thin sections, showing dark stromatolitic laminae (labeled "D" in d and f), light stromatolitic laminae (labeled "L" in d and f), and the dolomitic matrix (h). Yellow dashed lines in (c–f) denote boundaries between light and dark stromatolitic laminae. Blue arrows in (g) and (h) mark undolomitized calcite. (e) and (f) show the same area.

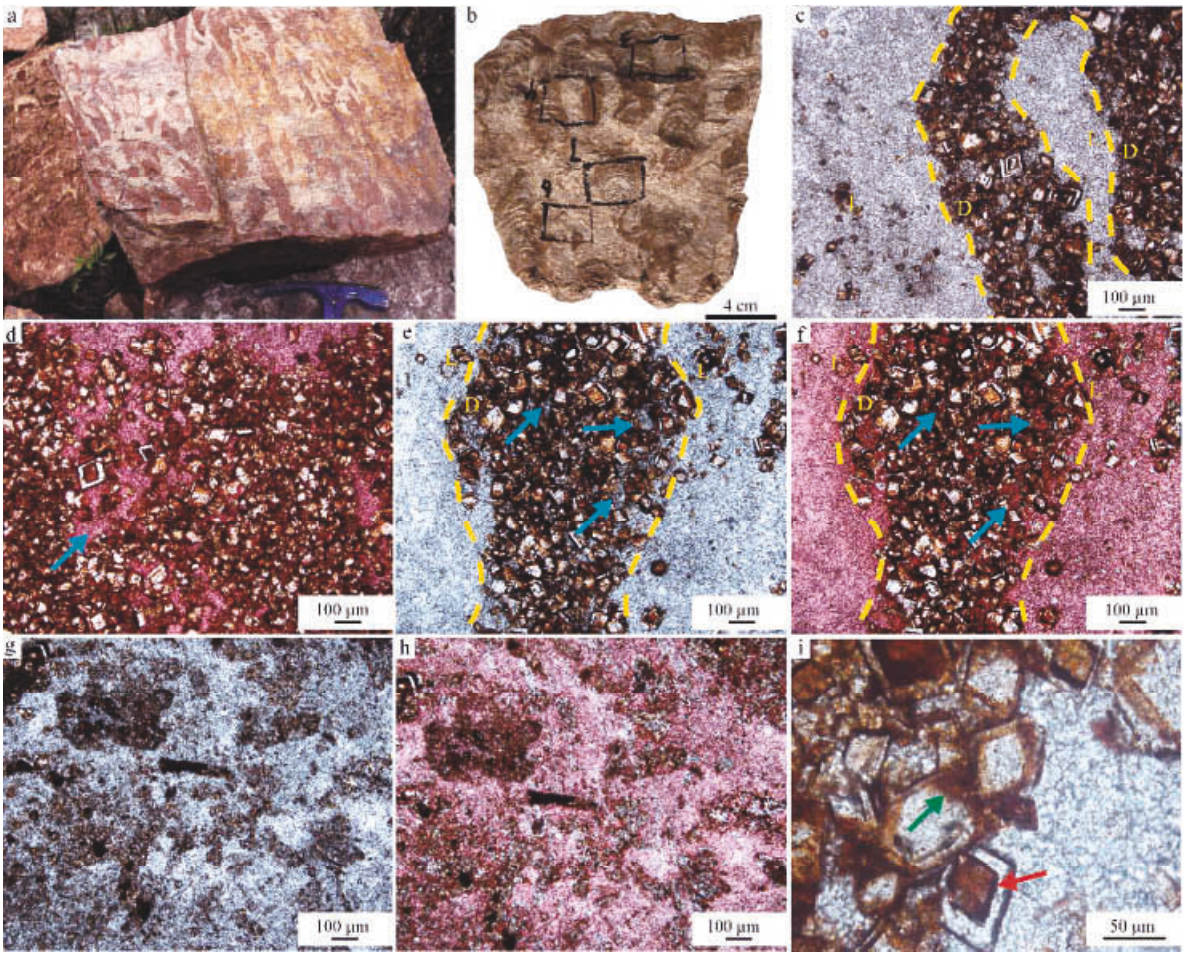

Fig. 3. Stromatolitic and dolomitic limestone with type II dolomitization pattern.
(a–b) Outcrop and hand-specimen photographs showing red-colored columnar stromatolites and light-gray matrix. Boxes in (b) mark areas selected to make thin and thick sections; (c, e, g) transmitted light photomicrographs of petrographic thin sections, showing that the dark-colored stromatolitic laminae (labeled "D" in c, e) are preferentially dolomitized, whereas light-colored stromatolitic laminae (labeled "L" in c, e) and the matrix (g) consist largely of sparry calcite. Syntaxial ferroan dolomite (red) and non-ferroan dolomite (transparent) overgrowth bands are well developed within the dark laminae (c, e); (d, f, h) transmitted light photomicrographs of ARS-stained thin sections, showing dark stromatolitic laminae (d and labeled "D" in f), light stromatolitic laminae (labeled "L" in f), and the matrix (h). Yellow dashed lines in (c, e, f) mark boundaries between light and dark laminae. Blue arrows in (d, e, f) mark sparry calcite within dark laminae. (e–f) and (g–h) are pairs of images showing the same areas; (i) overgrowth bands of dolomite crystals in dark stromatolitic laminae. Red and green arrows in (i) denote clear (red) and cloudy (green) boundaries between bands or between growth bands and the core.

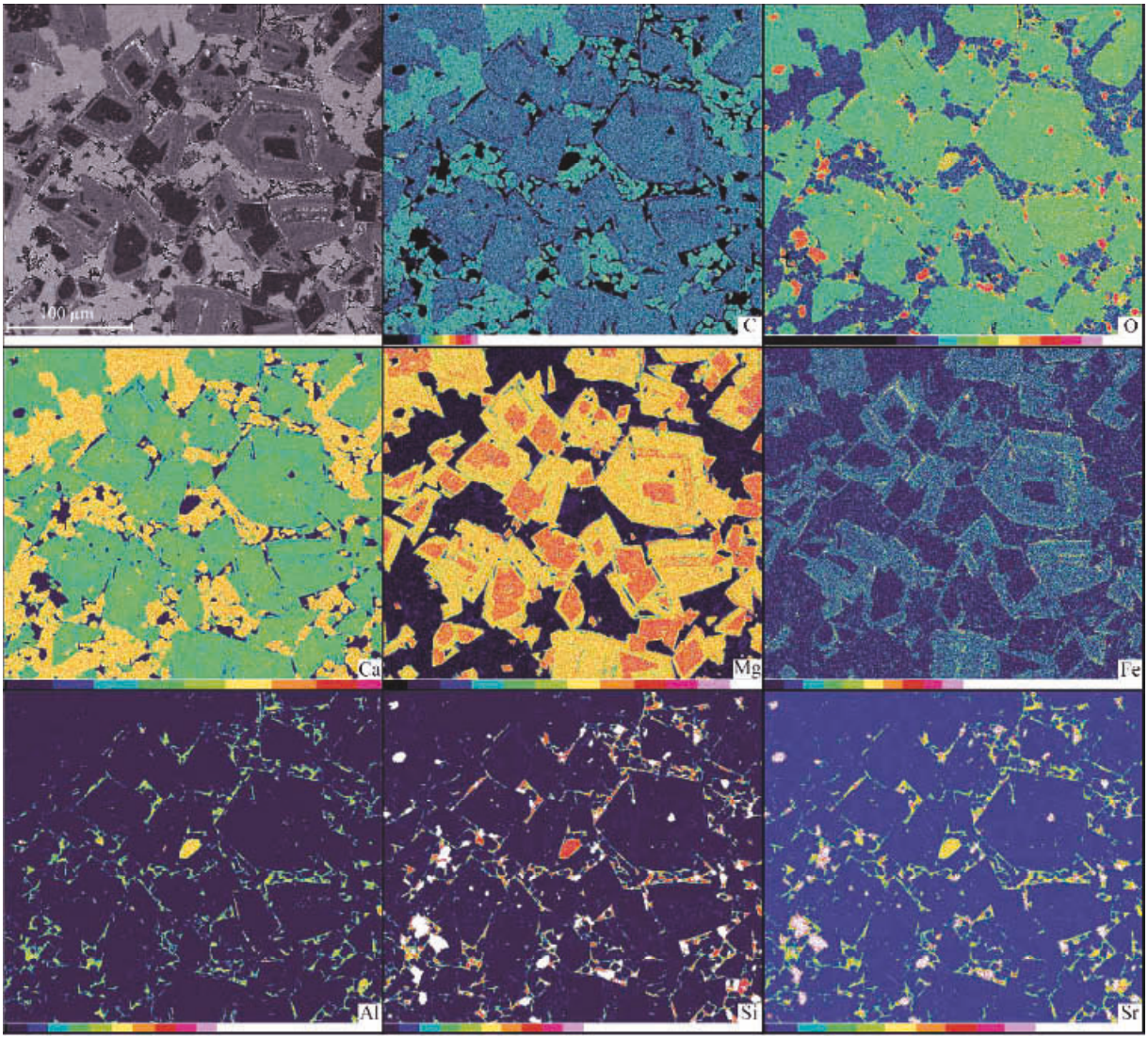

Fig. 4. BSE image (top left panel) and EDS elemental maps (elements labeled in the lower right of each panel) of rhombic dolomite crystals in dark stromatolitic laminae in dolomitic limestones with type II dolomitization pattern.
For rhombic dolomite crystals in the BSE image, the brightest (white) thin bands are red ferroan overgrowth bands, other darker bands are transparent non-ferroan overgrowth bands.

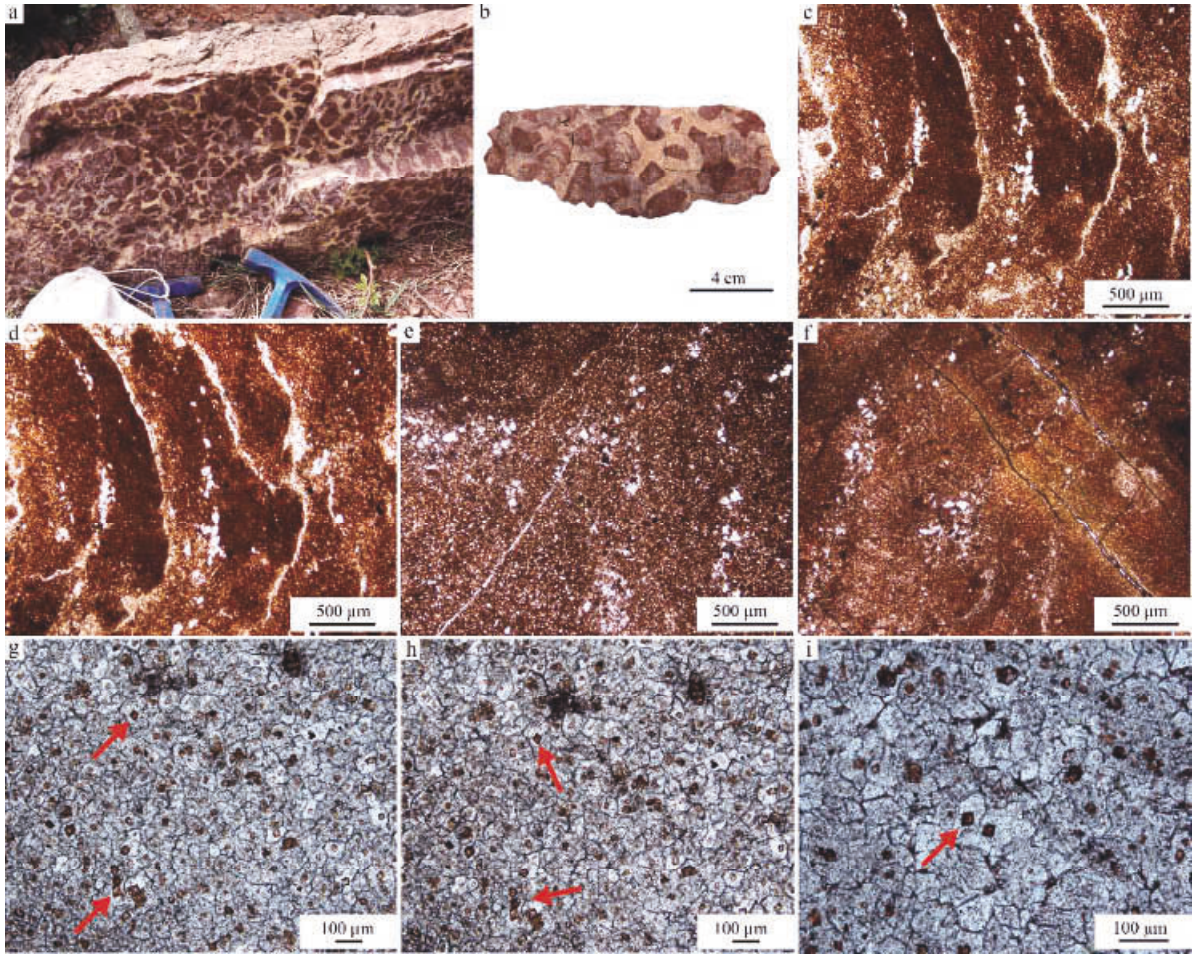

Table 1 Average concentrations of major and minor element concentrations, and average $\delta^{18}O$ and $\delta^{13}C$ values of dolomitic limestones and dolostones with three types of dolomitization (one-standard-deviations are presented)

Dolomitization pattern		Carbonate (wt%)	Mg/Ca	Fe (ppm)	Mn (ppm)	Sr (ppm)	δ O (‰)	δ C (‰)
Type I	Dark laminae (n = 12)	86.8 ± 4.4	0.012 ± 0.001	629.2 ± 129.3	651.7 ± 102.3	176.7 ± 12.8	−5.85 ± 0.45	2.75 ± 0.12
	Light laminae (n = 12)	87.9 ± 8.6	0.011 ± 0.001	428.1 ± 236.5	666.1 ± 123.3	180.4 ± 15.0	−5.32 ± 0.67	2.76 ± 0.12
	Mixture of dark and light laminae (n = 3)	88.6 ± 3.7	0.016 ± 0.005	1034.4 ± 691.3	609.3 ± 106.9	156.5 ± 54.5	−6.11 ± 1.53	2.36 ± 0.63
	Matrix (n = 5)	77.3 ± 7.7	0.20 ± 0.19	2209.4 ± 1555.4	1321.3 ± 597.4	136.0 ± 29.4	−5.88 ± 1.48	2.40 ± 0.83
Type II	Dark laminae (n = 5)	83.8 ± 4.0	0.27 ± 0.10	16465.8 ± 5528.2	2512.7 ± 747.5	106.2 ± 13.4	−6.26 ± 0.38	1.31 ± 0.25
	Light laminae (n = 5)	87.5 ± 2.0	0.06 ± 0.01	4999.0 ± 824.0	921.9 ± 82.7	107.0 ± 3.1	−6.98 ± 0.17	1.19 ± 0.04
	Mixture of dark and light laminae (n = 8)	85.7 ± 3.9	0.23 ± 0.09	14985.9 ± 6468.7	2310.0 ± 791.5	108.0 ± 9.5	−6.37 ± 0.29	1.37 ± 0.09
	Matrix (n = 7)	88.8 ± 5.4	0.13 ± 0.18	6369.6 ± 5695.1	1284.2 ± 1306.2	117.1 ± 11.2	−6.66 ± 0.90	1.23 ± 0.21
Type III	Stromatolite (n = 9)	74.6 ± 4.0	0.83 ± 0.06	3758.7 ± 1047.6	1327.7 ± 281.4	82.9 ± 11.5	−4.41 ± 0.31	−0.73 ± 0.40
	Matrix (n = 10)	74.8 ± 4.9	0.85 ± 0.03	3782.1 ± 568.1	1160.5 ± 231.5	83.4 ± 8.7	−4.58 ± 0.22	−0.63 ± 0.46

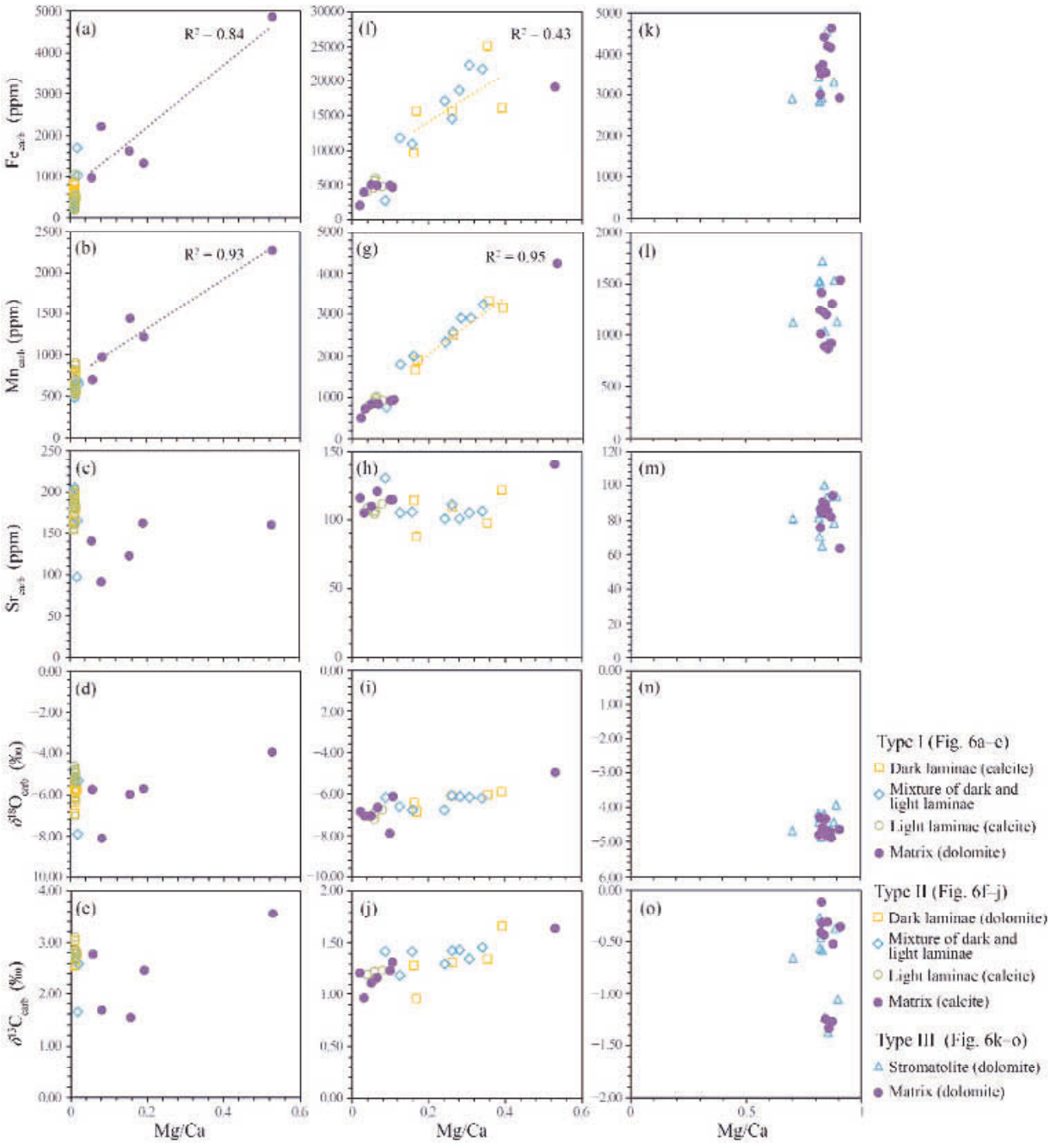

Fig. 6. Cross-plots showing the relationship between Mg/Ca and Fe_{carb}, Mn_{carb}, Sr_{carb}, $\delta^{18}O_{carb}$, and $\delta^{13}C_{carb}$ of dolomitic limestones with type I (a–e) and type II (f–j) dolomitization patterns, and dolostones with type III dolomitization pattern (k–o).
The regression lines of type I dolomitization are based on data of the matrix and those of type II dolomitization are based on data of dark stromatolitic laminae.

Table 2 Rare earth element, yttrium, and thorium concentrations (ppm) of dolomitic limestones and dolostones with three types of dolomitization

	Sample number		La	Ce	Pr	Nd	Sm	Eu	Gd	Tb	Dy	Y	Ho	Er	Tm	Yb	Lu	ΣREE	Th	Y/Ho	Eu/Eu*	Ce/Ce*	BSI
Type I	1-5	Light laminae	1.58	3.29	0.45	2.08	0.36	0.10	0.54	0.09	0.50	5.05	0.12	0.34	0.04	0.23	0.04	14.81	0.15	43.30	1.06	0.98	1.28
		Dark laminae	2.42	7.16	0.75	3.63	0.81	0.17	0.92	0.14	0.87	6.12	0.17	0.44	0.06	0.35	0.06	24.06	0.16	36.91	0.90	1.33	1.52
		Matrix	4.05	12.48	1.65	7.56	1.60	0.35	1.58	0.25	1.38	9.19	0.28	0.74	0.10	0.62	0.09	41.92	2.18	33.40	1.04	1.00	1.48
	1-6	Light laminae	3.01	8.70	1.06	4.69	1.04	0.21	1.00	0.16	0.90	6.88	0.18	0.47	0.06	0.46	0.07	28.90	1.38	37.62	0.99	1.06	1.42
		Dark laminae	3.61	12.46	1.58	7.29	1.67	0.34	1.58	0.25	1.32	8.30	0.26	0.70	0.09	0.59	0.09	40.14	2.28	32.26	0.98	1.06	1.57
Type II	3-1-1	Light laminae	1.23	3.16	0.47	2.21	0.54	0.10	0.54	0.09	0.49	4.11	0.10	0.33	0.04	0.27	0.04	13.72	0.34	39.27	0.85	0.92	1.37
		Dark laminae	1.71	4.84	0.71	3.45	0.83	0.17	0.92	0.14	0.83	5.92	0.15	0.45	0.06	0.34	0.05	20.58	1.43	39.30	0.91	0.94	1.63
	3-1-2	Light laminae	1.31	3.52	0.51	2.55	0.56	0.12	0.57	0.09	0.60	4.26	0.11	0.34	0.04	0.29	0.04	14.90	0.63	37.26	0.96	1.01	1.42
	3-1-3	Light laminae	1.38	3.93	0.52	2.18	0.49	0.11	0.54	0.08	0.54	3.94	0.11	0.29	0.05	0.28	0.04	14.46	0.54	37.05	1.01	0.92	1.36
		Dark laminae	1.76	5.56	0.76	3.43	0.87	0.17	0.77	0.15	0.80	5.71	0.16	0.46	0.06	0.31	0.05	21.02	1.70	35.55	1.00	0.94	1.53
		Matrix	1.21	2.86	0.42	1.95	0.44	0.10	0.50	0.08	0.53	4.07	0.10	0.33	0.04	0.25	0.04	12.92	0.49	42.56	0.96	0.91	1.39
	3-3-2	Light laminae	2.09	6.89	0.95	4.64	1.01	0.21	1.07	0.18	1.08	7.84	0.21	0.57	0.07	0.41	0.06	27.28	0.19	38.25	0.94	1.03	1.57
		Dark laminae	1.34	3.51	0.46	2.19	0.46	0.09	0.51	0.09	0.54	3.96	0.10	0.30	0.04	0.25	0.04	13.89	1.56	38.14	0.87	1.04	1.37
Type III	6-13	Stromatolite	3.57	12.10	1.68	9.09	2.95	0.64	3.47	0.54	2.99	19.91	0.55	1.58	0.20	1.25	0.18	60.69	1.88	35.93	0.93	1.13	1.89
		Matrix	3.29	12.11	1.90	10.40	3.70	0.80	3.99	0.60	3.34	19.73	0.58	1.60	0.19	1.17	0.17	63.56	1.52	33.94	0.97	1.01	2.17

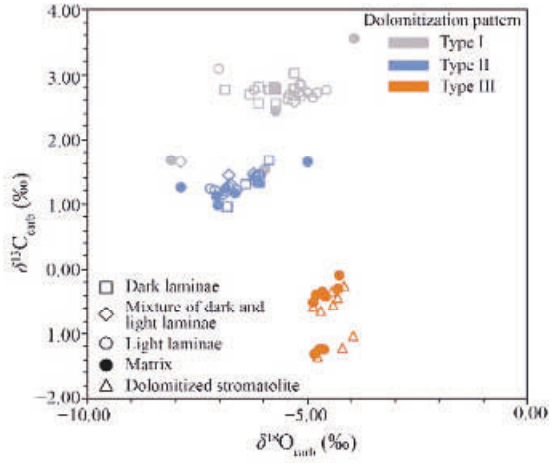

Fig. 7. Cross-plot of $\delta^{18}O_{carb}$ and $\delta^{13}C_{carb}$ of dolomitic limestones and dolostones grouped by different dolomitization patterns. Compared with dolomitic limestones with type I and type II dolomitization, dolostones with type III dolomitization show distinct $\delta^{18}O_{carb}$ and $\delta^{13}C_{carb}$ signals.

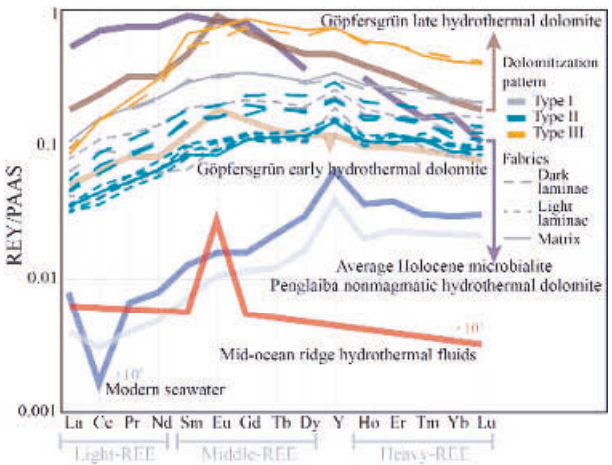

Fig. 8. Post-Archean Australian shale (PAAS) normalized rare earth elements and yttrium (REY) patterns of dolomitic limestones and dolostones grouped by different dolomitization patterns.

Fabrics are differentiated by the style of lines. Modern seawater, mid-ocean ridge hydrothermal fluids, average Holocene microbialite, and Göpfersgrün early and late hydrothermal dolomite REY patterns were adopted from Chang et al. (2020) and references therein. Penglaiba nonmagmatic hydrothermal dolomite REY patterns (no Eu anomaly) were adopted from Zhang et al. (2014).

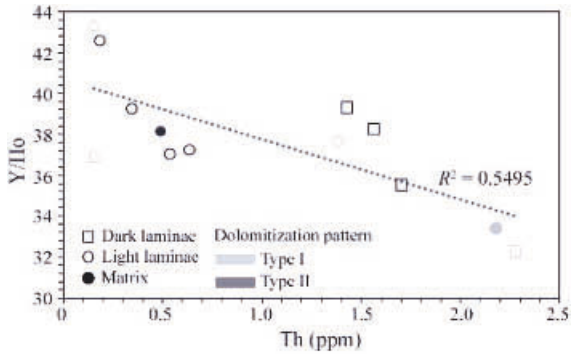
Y/Ho
Th (ppm)
R^2 = 0.5495
Dark laminae
Light laminae
Matrix
Dolomitization pattern
Type I
Type II